INTERNATIONAL JOURNAL OF CLIMATOLOGY
Int. J. Climatol. (2016)
Published online in Wiley Online Library
(wileyonlinelibrary.com) DOI: 10.1002/joc.4635

RMetS
Royal Meteorological Society

Spatiotemporal variation of temperature, precipitation and wind trends in a desertification prone region of China from 1960 to 2013

Zhongjie Shi,[a] Nan Shan,[a] Lihong Xu,[b] Xiaohui Yang,[a]* Jixi Gao,[c]* Hao Guo,[a] Xiao Zhang,[a] Aiyun Song[d] and Linshui Dong[d]

[a] *Institute of Desertification Studies, Chinese Academy of Forestry, Beijing, China*
[b] *Institute of Forest Ecology, Environment and Protection, Chinese Academy of Forestry, Beijing, China*
[c] *Nanjing Institute of Environmental Sciences, Ministry of Environmental Protection, Nanjing, China*
[d] *Key Laboratory of Eco-Environmental Science for Yellow River Delta of Shandong Province, Binzhou University, Binzhou, China*

ABSTRACT: Spatial and temporal distributions of temperature, precipitation and wind speed from 1960 to 2013 at 179 meteorological stations situated in the desertification prone region (DPR) of China are analysed using the Mann–Kendall test and the Theil–Sen's slope estimator on monthly, seasonal and annual timescales. The results indicate that annual mean temperature has increased at a rate of 0.33 °C (10 year)$^{-1}$ over the DPR. T_{min} generally increased at a higher rate than T_{max} in the majority of the months and seasons over the past 54 years; this has resulted in a decrease in the diurnal temperature range. Precipitation increased for the majority of the meteorological stations in the western area of the DPR, and decreased in the eastern area, but few of these trends are statistically significant on all timescales. The majority of meteorological stations recorded a significant decrease in wind speed at the majority of timescales. Results from this investigation show that the climate is becoming warmer and wetter in the western area of the DPR, and warmer and drier in eastern area of the DPR. A greater understanding of how the historical climate has been changing enables scientific support for the adaption of mitigation policies for land desertification/degradation, water resources, ecological projects and agricultural production. These policies will aid in combating the desertification processes, maintaining ecological security and promoting sustainable development in the DPR.

KEY WORDS temperature; precipitation; wind speed; trend; desertification; China

Received 7 August 2015; Revised 3 December 2015; Accepted 3 December 2015

1. Introduction

Climate change is one of the greatest challenges facing humanity since the industrial revolution. Near-surface global mean air temperatures have increased by 0.72 °C between 1951 and 2012 (IPCC, 2013), and mean global annual land precipitation has exhibited a slight increasing trend of approximately 1.1 ± 1.5 mm per decade between 1901 and 2005 (Trengberth *et al.*, 2007). Near-surface global annual average wind speed has also decreased by 0.014 m s^{-1} (McVicar *et al.*, 2012). However, there are large regional differences in the changes of these climatic variables. It has been recognized that global or continental-scale observations of historical climate are not very useful for local or regional planning and management (Martinez *et al.*, 2012). Greater attention has been placed on the historical trends in local or regional near-surface climate to adapt and mitigate the potential impacts of climate change (Dai *et al.*, 2015). A better evaluation of historical trends and spatial variations on a regional or local scale is therefore essential for hydrological, agricultural, and ecological management, as well as for policy-makers.

The desertification prone region (DPR) is a fragile ecological area which is susceptible to land desertification and degradation in the north of China (Wu *et al.*, 2007). This area has a vegetation cover/land use which includes grassland, desert, and farmland. The region has suffered a series of serious land desertification/degradation episodes which have affected crop production and people's livelihood. To control desertification/degradation, many ecological restoration projects, such as grain to green, Three-North shelterbelt project, Beijing-Tianjin sandstorm source control project, and the Three-River-Source ecological protection project have been implemented. Recently, glacier retreat and snowline rise, melting permafrost, lake shrinkage, increasing natural hazards and drought have been observed in many areas, all of which are closely related to global change and have become major threats in the DPR. Many studies have shown that climate change has an important impact on crop production, water resources,

* Correspondence to: X. Yang, Institute of Desertification Studies, Chinese Academy of Forestry, 10 Huaishuju Road, Haidian District, Beijing 100091, China. E-mail: yangxh@caf.ac.cn; or J. Gao, Nanjing Institute of Environmental Sciences, Ministry of Environmental Protection, 8 Jiangwangmiao street, Nanjing 210042, China. E-mail: gjx@nies.org

land desertification/degradation, and ecological restoration projects in arid and semiarid regions (Yang *et al.*, 2013; Shan *et al.*, 2015). In the context of future climate change, policy-makers are increasingly unable to make decisions for land management, ecological restoration, crop production, and water resources using historical climate normality (Takle *et al.*, 2014; Dai *et al.*, 2015). A warming climate may lead to a higher risk of crop failure, a higher frequency of droughts, and stronger land desertification/degradation, therefore this region is considered to be sensitive to climate change.

Recently, changes in temperature, precipitation, and evapotranspiration (as well as other climatic variables) have been recorded across some regions of northern China; these changes have obvious trends and regional differences (Ren and Yang, 2007; Lu *et al.*, 2009; Yang *et al.*, 2013; Shan *et al.*, 2015; Song *et al.*, 2015). However, little information is available on climate change in the DPR. Trends in temperature, precipitation, and wind speed will have greater impacts on land desertification/degradation, the occurrence of sandstorms, changes to regional water resources, ecological impacts, and the effect on crop production (Lobell and Burke, 2008; Wang *et al.*, 2010; Yang *et al.*, 2013). A better understanding of the magnitude of climatic variables is one of the most important aspects for climate change impact assessments and adaptation processes for land and water resource management, the implementation of ecological projects, and agricultural production. The objectives of our study are to investigate the trends in maximum (T_{max}), minimum (T_{min}), mean (T_{mean}) temperatures; the diurnal temperature range (DTR); precipitation (P); and wind speed (WS) on monthly, seasonal and annual timescales, and their spatial changes between 1960 and 2013 across the DPR. This will lead to a better understanding of how climate has been changing in the DPR, and it will provide scientific support for the adaption of mitigation policies of land desertification/degradation, water resource, ecological projects, and agricultural production.

2. Data and methods

2.1. Study area

The DPR, located in northern China (26°–47°N, 70°–128°E), covers approximately 4.54×10^6 km^2. This area includes the Xinjiang and Ningxia province; most parts of Inner Mongolia, Qinghai, Gansu and Tibet province; the northern part of Shannxi, Shanxi, and Hebei provinces; western Jilin province; and southwestern Heilongjiang province (Figure 1). The area has a complicated topography with altitudes between −154 and 8848 m, and includes basins, mountains, plateaus, and plains. The area, with a semi-humid to arid environment, has a temperate continental climate that is characterized by hot, wet summers and cold, dry winters. The majority of the DPR consists of deserts, grasslands, and cropland, these areas accounting for 42.9, 42.6, and 8.2% of this region, respectively. Deserts are largely distributed in the western area of the Helan Mountains and sand lands are largely concentrated in the eastern area of the Helan Mountains; these locations are the primary source for the majority of dust storms in China. Many farmlands were distributed in this region, such as Tarim river basin, Hetao-Ningxian plain, Western Liao river basin, Songnei sandland, etc. To the west of the DPR, in Northern Xinjiang and the Hexi corridor, the farmland in the oases are irrigated by the many inland rivers, such as Tarim river, Heihe river, with the main crops being wheat, corn, and potato. In the Xinjiang, Ningxia, and Gansu Provinces many economic crops and fruits with a higher quality, such as cotton, beet, grape, muskmelon, Chinese wolfberry, and pear are also produced. In the Hetao and Yinchuan plain, potato, wheat, corn and rice are irrigated by the Yellow River. The eastern farmland of the DPR is cultivated by precipitation or irrigation, and the main crops include corn and wheat. Due to the complex topography and climate, the region has been divided into three sub-regions: sub-region I is located in the eastern area of the Helan Mountains; sub-region II is located in the western area of the Helan Mountains; and sub-region III is located in the middle and northern part of the Tibet-Qinghai Plateau (Figure 1).

2.2. Data source

The China Meteorological Data Sharing Service System (http://cdc.cma.gov.cn) provided monthly meteorological data for the DPR spanning 1960–2013. The recorded meteorological variables included: (1) mean temperature (T_{mean}, °C); (2) mean maximum temperature (T_{max}, °C); (3) mean minimum temperature (T_{min}, °C); (4) precipitation (P, mm); (5) mean wind speed (WS, m s^{-1}); and (6) diurnal temperature range (DTR, °C), this being calculated as the difference between T_{max} *and* T_{min}. The data have been made a rigid quality control by China Meteorological Administration. As there were relatively few meteorological stations installed in Tibet in the 1960s, some stations which had data since the 1970s were used, these included Anduo, Gaize, Nimu, Nielamu, Lazi, Pulan, Dangxiong, and Shiquanhe meteorological stations. In total 179 meteorological stations were selected for this study (Figure 1). The meteorological stations were relatively well distributed over the DPR, however, the weather stations were less representative within the Taklimakan and Gurbantunggut Deserts, and on the Northern Tibetan Plateau. The seasons were divided into: spring (March to May); summer (June to August); autumn (September to November); and winter (December to February). The growing season was April to September.

2.3. Methods

To identify trends in temperature, precipitation, and wind speed between 1960 and 2013, the nonparametric Mann–Kendall (MK) test was applied (Kendall, 1975). This test has been widely used for trend testing of hydrological and meteorological data (Tabari and Hosseinzadeh Talaee, 2011; Martinez *et al.*, 2012; Yang *et al.*, 2013; Sayemuzzaman and Jha, 2014; Dai *et al.*, 2015;

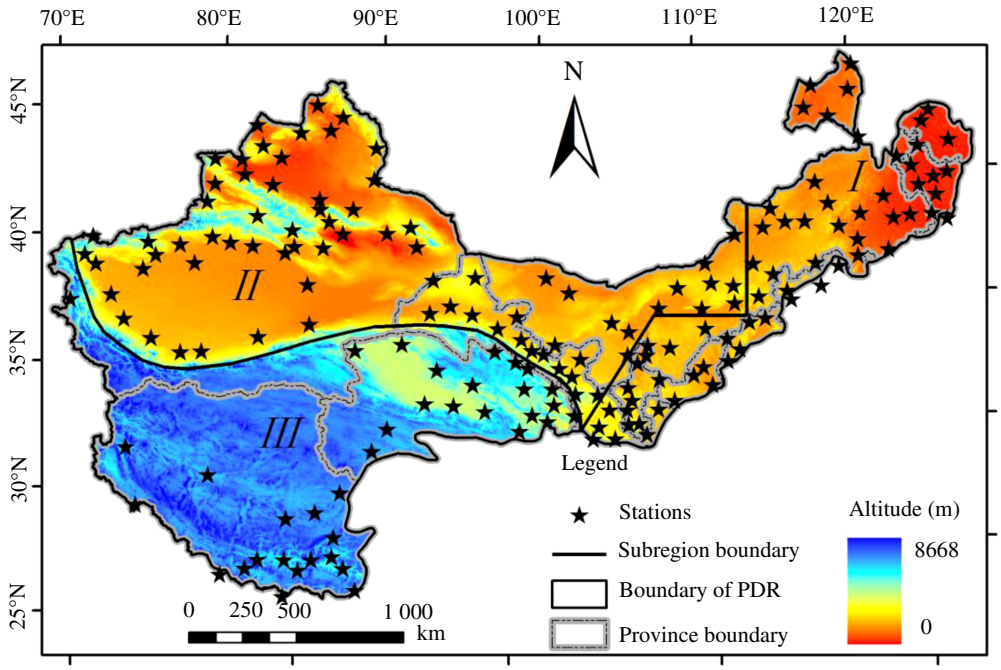

Figure 1. Location of the meteorological stations in the DPR.

Shan *et al.*, 2015). The nonparametric Theil-Sen's slope estimator was also used to estimate the slope of trends (Sen, 1968).

To evaluate the spatial distribution of trends in the climatic variables, the spline method was used to interpolate the variables. The spline method is characterized by fitting a smooth and continuous surface with the observation points and it did not need a preliminary estimate for the structure of temporal variance and statistical hypothesis (Zhu *et al.*, 2011) and has been widely used for the hydro-meteorological variables (Tait and Woods, 2007; Zhu *et al.*, 2011).

3. Results

3.1. Trends in T_{max} and T_{min}

Across the DPR, annual T_{max} and T_{min} trends between 1960 and 2013 were 0.26 ± 0.10 and $0.44 \pm 0.21\,^{\circ}\mathrm{C}\,(10\,\mathrm{year})^{-1}$, respectively. The statistically significant ($p < 0.05$) increasing trends in annual T_{max} and T_{min} have been detected for almost all of the meteorological stations (92.7 and 96.6% of stations, respectively) (Table 1). The highest warming was mainly located in the Qinghai-Tibet plateau, eastern Xinjiang and western Inner Mongolia (Figure 2(a) and (b)). During the growing season, T_{max} and T_{min} significantly increased by 0.23 ± 0.12 and $0.40 \pm 0.20\,^{\circ}\mathrm{C}\,(10\,\mathrm{year})^{-1}$, respectively, and were observed at 86.6 and 92.7% of stations. On seasonal timescales, most stations showed an increase in T_{max} and T_{min} for all the seasons (Table 1). The proportion of meteorological stations showing this trend for T_{max} was 54.7% in spring, 66.5% in summer, 81.0% in autumn, and 41.9% in winter, with an increase of 0.25, 0.20, 0.29, and $0.27\,^{\circ}\mathrm{C}\,(10\,\mathrm{year})^{-1}$, for the four seasons, respectively. However, the majority of meteorological stations (more than 86% of stations) showed a significant positive trend in T_{min} in all seasons. The greatest increase in T_{min} occurred in winter [$0.54\,^{\circ}\mathrm{C}\,(10\,\mathrm{year})^{-1}$] and the lowest values were in the summer [$0.39\,^{\circ}\mathrm{C}\,(10\,\mathrm{year})^{-1}$]. On a monthly timescale, the dominant trends in T_{max} and T_{min} showed an increase in all months. However, more stations recorded an increase in T_{min} than that in T_{max}. Over the period of 1960–2013, February was found to be the month with the greatest increase in T_{max} and T_{min} of 0.48 and $0.74\,^{\circ}\mathrm{C}\,(10\,\mathrm{year})^{-1}$, respectively (Figure 3(a) and (b)). The warming trend was lowest for T_{max} in January ($0.17\,^{\circ}\mathrm{C}\,(10\,\mathrm{year})^{-1}$) and T_{min} in August ($0.32\,^{\circ}\mathrm{C}\,(10\,\mathrm{year})^{-1}$) (Figure 3(a) and (b)). In addition, decreases in T_{max} were identified in January, July, and December, found in 23.5, 11.2, and 10.1% of the meteorological stations.

Between the different sub-regions, T_{max} and T_{min} increased, with the greatest increase in annual T_{max} and T_{min} found in sub-regions III ($0.30\,^{\circ}\mathrm{C}\,(10\,\mathrm{year})^{-1}$) and II ($0.48\,^{\circ}\mathrm{C}\,(10\,\mathrm{year})^{-1}$), respectively. However, the lowest increase in annual T_{max} and T_{min} was shown at sub-regions II ($0.24\,^{\circ}\mathrm{C}\,(10\,\mathrm{year})^{-1}$) and I ($0.38\,^{\circ}\mathrm{C}\,(10\,\mathrm{year})^{-1}$), respectively. In the growing season, similar differences in T_{max} and T_{min} were identified in the different sub-regions. On the seasonal timescale, T_{max} peaked in winter at sub-regions III and I (0.40 and $0.30\,^{\circ}\mathrm{C}\,(10\,\mathrm{year})^{-1}$, respectively), and in the autumn at sub-region II ($0.30\,^{\circ}\mathrm{C}\,(10\,\mathrm{year})^{-1}$). The increase in T_{max} in winter was twice as fast at sub-region III than that of the summer in sub-region II ($0.18\,^{\circ}\mathrm{C}\,(10\,\mathrm{year})^{-1}$). The seasonal increases in T_{min} were similar in sub-regions II and III, and larger than sub-region I. On the monthly timescale, the

Table 1. Statistic of annual and seasonal trends of T_{max} [°C (10 year)$^{-1}$], T_{min} [°C (10 year)$^{-1}$], T_{mean} [°C (10 year)$^{-1}$], DTR [°C (10 year)$^{-1}$], P (mm (10 year)$^{-1}$), and WS (m s (10 year)$^{-1}$) for the 179 stations in the DPR.

Timescale	Variable	Trend magnitude	Decreasing	Increasing	Timescale	Variable	Trend magnitude	Decreasing	Increasing
Annual	T_{max}	0.26 ± 0.10	1 (**0.6%**, *0.6%*)	178 (**99.4%**, *92.7%*)	Summer	T_{max}	0.20 ± 0.14	11 (**6.1%**, *1.1%*)	168 (**93.9%**, *66.5%*)
	T_{min}	0.44 ± 0.21	3 (**1.7%**, *0.6%*)	176 (**98.3%**, *96.6%*)		T_{min}	0.39 ± 0.21	7 (**3.9%**, *1.1%*)	172 (**96.1%**, *90.5%*)
	T_{mean}	0.33 ± 0.12	2 (**1.1%**, *0.0%*)	177 (**98.9%**, *97.2%*)		T_{mean}	0.26 ± 0.14	8 (**4.5%**, *1.7%*)	171 (**95.5%**, *88.3%*)
	DTR	−0.19 ± 0.20	155 (**86.6%**,*66.5%*)	24 (**13.4%**,*5.6%*)		DTR	−0.18 ± 0.18	151 (**84.4%**,*60.9%*)	28 (**15.6%**,*3.9%*)
	P	2.30 ± 8.38	64 (**35.8%**, *0.6%*)	115 (**64.2%**, *22.9%*)		P	−0.01 ± 6.24	80 (**44.7%**,*3.4%*)	99 (**55.3%**,*11.7%*)
	WS	−0.16 ± 0.14	163 (**91.1%**, *75.4%*)	16 (**8.9%**, *5.0%*)		WS	−0.14 ± 0.16	153 (**85.5%**, *65.9%*)	26 (**14.5%**, *5.6%*)
Growing season	T_{max}	0.23 ± 0.12	4 (2.2%, 1.1%)	175 (97.8%, 86.6%)	Autumn	T_{max}	0.29 ± 0.11	1 (**0.6%**, *0.0%*)	178 (**99.4%**, *81.0%*)
	T_{min}	0.40 ± 0.20	5 (**2.8%**, *0.6%*)	174 (**97.2%**,*92.7%*)		T_{min}	0.42 ± 0.25	5 (**2.8%**, *1.1%*)	174 (**97.2%**, *86.00%*)
	T_{mean}	0.28 ± 0.12	3 (**1.7%**, *0.6%*)	176 (**98.3%**, *93.3%*)		T_{mean}	0.33 ± 0.15	3 (**1.7%**, *1.1%*)	176 (**98.3%**, *92.2%*)
	DTR	−0.17 ± 0.18	153 (**85.5%**, *63.1%*)	26 (**14.5%**, *6.1%*)		DTR	−0.14 ± 0.25	130 (**72.6%**, *45.8%*)	49 (**27.4%**, *9.5%*)
	P	1.09 ± 7.43	73 (**40.8%**, *1.1%*)	106 (**59.2%**, *14.5%*)		P	0.03 ± 2.65	72 (**40.2%**, *2.8%*)	107 (**59.8%**, *6.7%*)
	WS	−0.16 ± 0.16	157 (**87.7%**, *72.6%*)	22 (**12.3%**, *5.0%*)		WS	−0.14 ± 0.14	158 (**88.3%**, *67.6%*)	21 (**11.7%**, *5.0%*)
Spring	T_{max}	0.25 ± 0.13	3 (**1.7%**, *0.0%*)	176 (**98.3%**, *54.7%*)	Winter	T_{max}	0.27 ± 0.18	7 (**3.9%**, *0.6%*)	172 (**96.1%**, *41.9%*)
	T_{min}	0.43 ± 0.21	3 (**1.7%**, *0.6%*)	176 (**98.3%**, *87.7%*)		T_{min}	0.54 ± 0.27	5 (**2.8%**, *0.0%*)	174 (**97.2%**, *86.0%*)
	T_{mean}	0.33 ± 0.12	2 (**1.1%**, *0.0%*)	177 (**98.9%**, *91.6%*)		T_{mean}	0.40 ± 0.17	2 (**1.1%**, *0.0%*)	177 (**98.9%**, *76.0%*)
	DTR	−0.19 ± 0.22	149 (**83.2%**, *60.3%*)	30 (**16.8%**, *4.5%*)		DTR	−0.29 ± 0.28	157 (**87.7%**, *66.5%*)	22 (**12.3%**, *2.8%*)
	P	1.04 ± 2.16	43 (**24.0%**, *0.6%*)	136 (**76.0%**, *11.7%*)		P	0.67 ± 1.18	22 (**12.3%**, *0.08%*)	157 (**87.7%**, *30.7%*)
	WS	−0.19 ± 0.17	165 (**92.2%**, *79.3%*)	14 (**7.8%**, *4.5%*)		WS	−0.14 ± 0.16	159 (**88.8%**, *67.6%*)	20 (**11.2%**, *5.6%*)

Percentage of stations (bold) and Percentage of stations with a significant ($p < 0.05$) trend (Italics) are indicated in parenthesis, for both negative and positive trends.

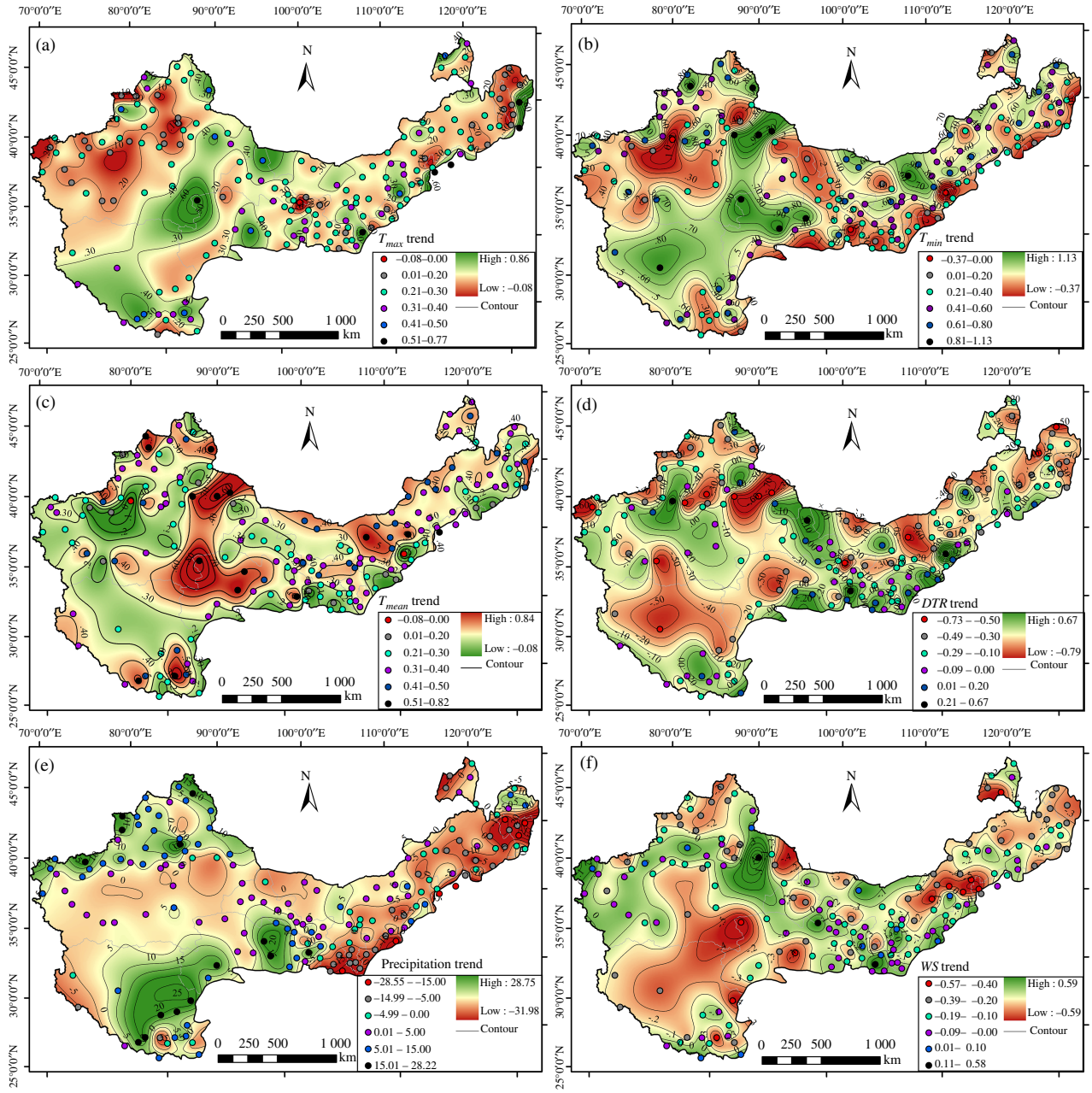

Figure 2. Distribution of trends in annual climatic variables during 1960–2013. (*a*) T_{max} [°C (10 year)$^{-1}$], (b) T_{min} [°C (10 year)$^{-1}$], (c) T_{mean} [°C (10 year)$^{-1}$], (*d*) DTR [°C (10 year)$^{-1}$], (e) *P* [mm (10 year)$^{-1}$], (*f*) WS (m s^{-1} (10 year)$^{-1}$).

differences between the sub-regions were greater in the cold months, such as January, November, and December.

3.2. Trends in T_{mean} and DTR

Annual mean temperatures have increased by 0.33 ± 0.12 °C (10 year)$^{-1}$ since 1960 in the DPR, and 97.2% of meteorological stations showed a significant increase at the 0.05 significance level (Table 1). The highest increasing trends in T_{mean} were mainly located in the Northwestern Qinghai-Tibet plateau, eastern Xinjiang and the middle of Inner Mongolia (Figure 2(c)). During the growing season, 93.3% of the meteorological stations showed a significant increase in T_{mean} of 0.28 ± 0.12 °C (10 year)$^{-1}$ (Table 1). For seasonal timescales, almost all stations recorded a positive trend in T_{mean} for all of the seasons (Table 1). In winter, 76.0% of meteorological stations recorded a significant increase in T_{mean} with a value of 0.40 °C (10 year)$^{-1}$. In summer, the lowest increase [0.26 °C (10 year)$^{-1}$] was recorded at 88.3% of meteorological stations with a significant increase. Over the spring and autumn, the warming trend was as high as 0.33 °C (10 year)$^{-1}$. The increases in the monthly T_{mean} records were recorded for all months (Figure 3(c)). The greatest warming trend in the T_{mean} occurred in February with 0.60 °C (10 year)$^{-1}$, almost 2.5 times as fast as the lowest increase [0.23 °C (10 year)$^{-1}$] recorded in August (Figure 3(c)). Totally 83.8 and 85.5% of meteorological stations recorded a significant increase

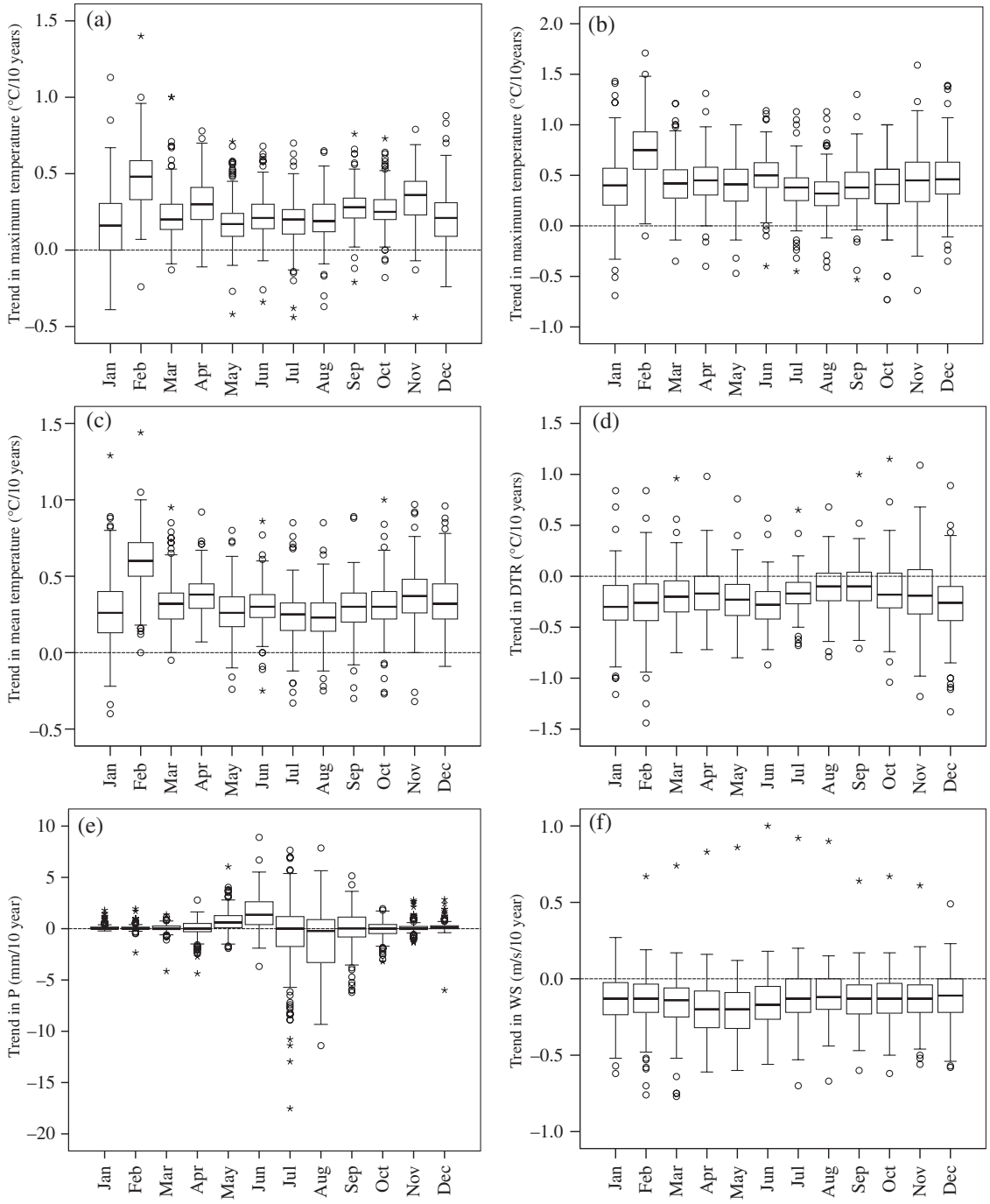

Figure 3. Box-and-whisker plots of trends in monthly climatic variables, 1960–2013. (a) T_{max} [°C (10 year)$^{-1}$], (*b*) T_{min} [°C (10 year)$^{-1}$], (c) T_{mean} [°C (10 year)$^{-1}$], (d) DTR [°C (10 year)$^{-1}$], (*e*) *P* (mm (10 year)$^{-1}$), (f) WS (m s (10 year)$^{-1}$).

in T_{mean}. Overall, the difference in the trends is small among the different sub-regions, but the greatest values mainly occur in sub-region III.

During 1960–2013, annual DTR trends decreased with a composite trend of 0.19 °C (10 year)$^{-1}$ (Table 1). Totally 86.6% of meteorological stations observed a negative trend and 66.5% of the meteorological station records were statistically significant. The greatest decreasing trends in DTR were mainly located in the northern Qinghai-Tibet plateau, eastern Xinjiang and the middle of Inner Mongolia (Figure 2(d)). During the growing season, DTR decreased by 0.17 ± 0.18 °C (10 year)$^{-1}$, and significant negative and positive trends in DTR were observed at 63.1 and 6.1% of stations, respectively. On a seasonal timescale, most of stations recorded the decrease in DTR across all seasons (Table 1). The greatest change for DTR occurred in winter, when T_{min} increased twice as fast as T_{max} (Table 1). On the monthly timescale, DTR series decreased for all months (Figure 3(d)). The greatest percentage of stations with significant decreases in monthly DTR were recorded in June (67.0%), with the lowest percentage being in August (29.1%). The greatest decrease in DTR occurred in January

[0.28 °C (10 year)$^{-1}$] when T_{min} increased 2.4 times as fast as T_{max}. The lowest decrease occurred in August with a value of 0.10 °C (10 year)$^{-1}$ (Figure 3(d)). In almost all timescales, DTR had the greatest negative trend in sub-region II.

3.3. Trends in precipitation

In the DPR, annual P increased by 2.30 ± 8.38 mm (10 year)$^{-1}$ between 1960 and 2013. Totally 64.2% of meteorological stations was observed an increase in annual P, and records from 22.9% of these meteorological stations were statistically significant (Table 1). The increasing trends were mainly distributed in the western area of the Helan Mountains (Figure 2(e)). However, decreases in P were mainly observed in the eastern areas of the Helan Mountains (Figure 2(e)). On average, P showed a positive trend of 7.94 mm (10 year)$^{-1}$ in sub-region III, and 5.74 mm (10 year)$^{-1}$ in sub-region II. Sub-region I had a negative trend of 4.77 mm (10 year)$^{-1}$. During the growing season, 59.2% of meteorological stations recorded increasing P, however, only 14.5% were statistically significant (Table 1), with a mean magnitude of 1.09 mm (10 year)$^{-1}$. The spatial distribution of growing season in trends also showed similar patterns to that of annual trends.

On the seasonal basis, P recorded a positive trend, except for the summer (Table 1), with 76.0, 55.3, 59.8, and 87.7 of meteorological stations showing a wetter trend in the spring, summer, autumn, and winter P series, respectively. Of these seasons, however, only 11.7%, 11.7%, 6.7%, and 30.7% of the meteorological stations observed statistically significant trends at the 0.05 level (Table 1). It is worth noting that spring and winter wetter trends were found in the eastern areas of the Helan Mountains, which is opposite to the summer and autumn trends. The composite increases were 1.04 and 0.67 mm (10 year)$^{-1}$ in spring and winter, respectively, but there was less variation in summer and autumn (Table 1). The positive trend was recorded in all seasons at sub-regions II and III, but a negative trend was found during the summer and autumn at sub-region I.

On the monthly timescale, the majority of the meteorological stations recorded January, February, May, June, November, and December to be wetter and July, August, and October to be drier; with no change in March, April, and September. Overall, the greatest drying trend occurred in August [−1.05 mm (10 year)$^{-1}$] when 59.2% of meteorological stations recorded the climate to be becoming drier (7.3% being statistically significant) (Figure 3(e)). The greatest wetting trend occurred in June [+1.62 mm (10 year)$^{-1}$] when 86.0% of meteorological stations recorded the climate to become wetter (13.4% being statistically significant). At sub-regions II and III, almost all months saw an increase in P, except August at sub-region II and October, November, and December at sub-region III with a slight decrease of P. However, a slight increase in P was identified in January, February, March, May, June, and December, and other months were shown to reflect decreasing P.

3.4. Trends in wind speed

Across the DPR the composite trends in annual WS between 1960 and 2013 were 0.158 ± 0.145 m s^{-1} (10 year)$^{-1}$ (Table 1). Totally 91.1% of meteorological stations recorded a decrease in annual WS, with 75.4% being statistically significant, scattered throughout the region. The greatest decreasing trends in WS were mainly located in the Qinghai-Tibet plateau, and the middle of Inner Mongolia (Figure 2(f)). During the growing season, WS decreased by 0.164 ± 0.154 m s^{-1} (10 year)$^{-1}$, and this decrease was observed at 87.7% of meteorological stations, with 72.6% being statistically significant. In seasonal timescales, the majority of the meteorological stations recorded a negative trend in WS for all of the seasons (Table 1). Spring WS series showed the greatest negative trends reaching 0.193 m s^{-1} (10 year)$^{-1}$, and 92.2% of the meteorological stations recorded decreasing WS (79.3% being statistically significant). Decreases of approximately 0.14 m s^{-1} (10 year)$^{-1}$ were observed in the summer, autumn, and winter, with 65.9, 67.6, and 67.6% of the meteorological stations showing this trend in summer, autumn, and winter, respectively (Table 1). On a monthly timescale, WS series showed negative trends for all months in approximately 60% of the meteorological stations (Figure 3(f)). The greatest decreases occurred in May and April, with values of 0.21 and 0.19 m s^{-1} (10 year)$^{-1}$, respectively; which 91.6 and 89.9% of the meteorological stations recorded this decrease (76.5 and 73.2% being significant, respectively).There was no obvious difference for WS at most timescales for the different sub-regions.

3.5. Comprehensive analysis

From 1960 to 2013, the majority of the meteorological stations across the DPR recorded a significant increase in air temperature. In the western area of the Helan Mountains (sub-regions II and III), an increase in precipitation was also recorded at most of the meteorological stations; the combination of the temperature and precipitation changes reflected a warmer and wetter climate which improved the arid environment in this area. However, precipitation records decreased for most of the meteorological stations in the eastern area of the Helan Mountains (sub-region I), which reflected the climate in this sub-region to be warmer and drier, thus being detrimental to the original arid environment of this area. With WS being recorded as significantly decreasing across all timescales for the majority of the weather stations, this implies that the atmosphere was becoming more stilling.

4. Discussion

The majority of meteorological stations in the DPR recorded positive trends in T_{max}, T_{min}, and T_{mean} at most timescales between 1960 and 2013. It was found that annual T_{max}, T_{min}, and T_{mean} increased by 0.26, 0.44, and 0.33 °C (10 year)$^{-1}$, respectively. These warming trends concur with temperature results from other investigations (Tabari and Hosseinzadeh Talaee, 2011; Martinez *et al.*,

2012; Duhan *et al.*, 2013; Yang *et al.*, 2013; Dai *et al.*, 2015; Najafi *et al.*, 2015). However, the magnitude of the increase in temperature from this investigation is generally higher than those from investigations from other parts of the world (Martinez *et al.*, 2012; Duhan *et al.*, 2013; Dai *et al.*, 2015). The positive trend for $T_{\min}$ was greater than the positive trend for $T_{\max}$ which has resulted in a decrease of DTR recorded at the majority of the meteorological stations in the DPR. The increasing air temperature were due to several factors, such as increasing anthropogenic greenhouse gas emissions and aerosols, increased cloud cover, and increasing urbanization (Najafi *et al.*, 2015).

In our study, precipitation records showed increases in sub-regions II [5.74 mm (10 year)$^{-1}$] and III [7.94 mm (10 year)$^{-1}$], and decreases in sub-region I [4.77 mm (10 year)$^{-1}$]. In previous studies in northwest China, annual precipitation has been recorded to show an obvious increase over the past 50 years (Chen *et al.*, 2011; Dai *et al.*, 2013; Song *et al.*, 2015), but an opposite trend has been identified for northeast China (He *et al.*, 2013; Song *et al.*, 2015). In addition, precipitation records between 1971 and 2000 showed a positive trend in the eastern parts of the Tibetan Plateau with negative trends in the western parts of the Plateau (Du and Ma, 2004). These results have a similar pattern to our result in the DPR. Due to the large area of the DPR, mechanisms affecting climate may change in the different regions. Wang *et al.* (2011) suggested that annual precipitation had a positive trend in the monsoon areas, yet results from this study showed a decrease in precipitation was recorded in sub-region I which is located in the marginal zone of the Eastern Asian Summer Monsoon (EASM). Within sub-region I, precipitation is closely related to the intensity of the EASM (Liu *et al.*, 2004; Sperber *et al.*, 2013), and the negative trend in precipitation may be due to a weakened EASM (Wang and Zhou, 2005; Ding *et al.*, 2008; Zhao *et al.*, 2010). This implies that stronger droughts are shifting towards the south and the east in sub-region I. In the southern part of sub-region III, the climate was controlled by the South Asian Summer Monsoon (SASM). The enhanced SASM (Hua *et al.*, 2012) may be the reason for increased precipitation in this region. In sub-region II and northern parts of sub-region III, the climate is a non-monsoon type, affected mainly by the Westerly, and precipitation is closely related to the intensity of the North Atlantic Oscillation (NAO) (Dai *et al.*, 2013). The wetter tendency of this region can be related to the enhanced NAO since 1960 (Gong and Wang, 2000; Chen *et al*, 2011). The positive trend was more obvious in the northern area of the Tianshan Mountains in our study. In addition, increased precipitation may also be affected by an enhanced hydrological cycle due to agricultural irrigation in the oasis (Zhu *et al.*, 2014). Moreover, precipitation variability may also be affected by the complex topography in the DPR.

Decreases in WS have also been identified in many regions across the globe (Hoffman *et al.*, 2011; McVicar *et al.*, 2012). In our study, WS recorded a significant decrease for most of the meteorological stations across the different timescales. The WS in the spring were identified as the most obvious negative trend in the DPR; reasons for decreasing WS may be due to a number of factors. Zhang *et al.* (2009) proposed that weaker large-scale atmospheric circulation associated with global warming is causing a decrease in WS, while Tubi and Dayan (2013) suggest that a weakened Siberian High is a possible cause. Declining temperature gradients between the polar and tropical regions, coupled with a weakening of the East Asian Monsoon (Xu *et al.*, 2006) are also believed to reduce the strength of atmospheric circulation and WS (McVicar *et al.*, 2012). In the western area of the DPR, the variation of WS was mainly due to the weakening of Cold High Pressure and cyclone activities (Japay and Gang, 2008). In addition, an increase in land surface roughness due to grain-for-green, afforestation, reforestation, and urbanization may also be a cause of decreasing WS (Vautard *et al.*, 2010). Due to the number of factors and influences that will affect WS, this area requires further research.

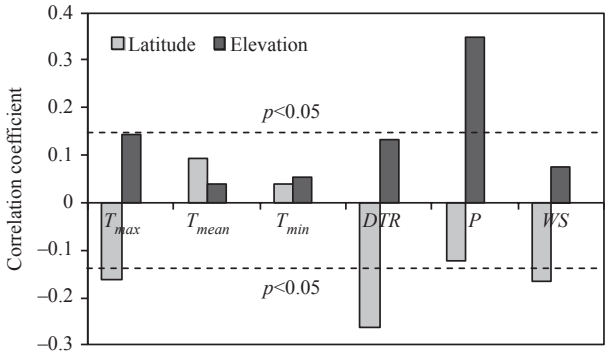

Figure 4. Correlation between the trend magnitudes in the climatic variables and latitude, elevation.

In addition, due to the large climate variation and complex landform, they may affect the variation of trends in the climatic variables. The correlation analysis showed the station elevation had a significantly positive correlation with the trends of precipitation ($p < 0.05$) and $T_{\max}$ ($p < 0.1$), suggesting the trends of precipitation and $T_{\max}$ had the larger increment at high altitudes (Figure 4). The latitude was significantly negative correlated with the trends of $T_{\max}$ ($p < 0.05$), DTR ($p < 0.05$) and WS ($p < 0.05$), suggesting these trends decrease with increasing latitude (Figure 4).

The DPR is recognized as a major source of dust for the frequently occurring dust storms during the spring months, and this is especially prevalent in sub-region II. Dust storms typically occur with strong winds, low vegetation cover, and low soil moisture conditions (Tan *et al.*, 2012). In our study area, WS recorded a significant decrease across all timescales; 92.2% of the meteorological stations recorded this decrease in WS in spring with 79.3% being statistically significant. The greatest decrease was 0.193 m s^{-1} (10 year)$^{-1}$ which may lead to a reduction in the frequency and intensity of dust storms. Although increasing air temperatures usually result in increasing evapotranspiration, Shan *et al.* (2015) and Li *et al.* (2014)

showed that evapotranspiration has reduced more significantly as a result of reductions in WS than increases in air temperature. Moreover, increasing precipitation and decreasing evapotranspiration in the spring and winter months across the DPR may have resulted in an increase in soil moisture, which may have impeded the occurrence of dust storm events in the spring. Although precipitation decreased in the eastern parts of the DPR, evapotranspiration decreased more significantly than precipitation (Shan *et al.*, 2015). Soil moisture may therefore not have decreased significantly, or it may even have experienced a slight increase, which may not be conducive to the formation of dust storms. A warming climate will advance spring phenology which will result in vegetation growth beginning earlier in the season, which may further impede the occurrence of dust storms (Fan *et al.*, 2014). Wang *et al.* (2010) reported that dust storm day occurrence decreased in the mid-1960s through the end of the 1990s; after which there was a slight increase recorded for dust storm days. The slight increase towards the end of the 1990s is related to the changes in precipitation and WS in the spring and winter months, a finding also supports the results from this study.

In the DPR, land desertification/degradation is a serious issue due to human activities and climate change (Wang *et al.*, 2006; Gao and Liu, 2010). To improve the fragile ecological environment, many ecological projects have been undertaken in this area. These include grain for green, Three-north shelterbelt, Beijing-Tianjin sand source control, afforestation, and reforestation. Soil water shortage, however, is the main limiting factor for these projects. In the western areas of the DPR (i.e. sub-regions II and III), precipitation increased at most of the meteorological stations, especially in northern Xinjiang. This increase may reduce the occurrence of drought events and result in an increase of soil moisture, thus promoting the performance of regional vegetation restoration and ecological projects, and reducing the impact of desertification/degradation. In the Tibet-Qinghai plateau (sub-region III), increasing air temperatures have accelerated the thawing of permafrost which has lead to the land degradation (CCNARCC, 2007). However, in the eastern part of the DPR, a reduction in precipitation was recorded in most of the permafrost stations, implying that droughts may start to occur more frequently. Increasing drought episodes may restrict the performance of ecological projects, and may even induce vegetation degradation and land desertification.

Under the context of climate change, the terrestrial hydrological cycle is being altered across the DPR. However, the effect of climate change differs between the different sub-regions. In sub-regions II and III, most of the area is in the inland river basin, such as Tarim, Heihe, Shiyang rivers, which are strongly reliant on the glaciers. Climate warming will accelerate the glacial ablation, thus further increasing runoff and glacier shrinkage (Wang *et al.*, 2015). In the Tibetan plateau (sub-region III), lake surface areas have significantly increased (Li, 2012) due to climate warming. Totally 82.2% of glaciers have shrunk and their surface areas have reduced by 4.5% in the past 50 years (Liu *et al.*, 2006). Alarmingly, glacial surface areas have also decreased by 21% in northwest China (CCNARCC, 2007). Increasing precipitation, runoff, and glacial ablation are the main hydrological components experiencing an accelerating trends, suggesting stronger hydrological cycles in sub-regions II and III. However, river runoff has also been observed to decrease in sub-region I (Zhang *et al.*, 2011; Guo *et al.*, 2014). Decreasing precipitation and runoff implies a weaker hydrological cycle in this sub-region which has led to the shrinkage of lake areas and volume (Liu *et al.*, 2013; Tao *et al.*, 2015).

In agricultural production, it is necessary to have a larger DTR which helps to increase crop production and improve crop quality (CCNARCC, 2007). Higher T_{max} and stronger sunlight can enhance plant photosynthesis and increase biomass production (yields); lower T_{min} can reduce plant respiration and nutrient consumption. Higher DTR, therefore, is conducive to the accumulation of biomass (Lobell, 2007; Yu *et al.*, 2014). In particular, lower T_{min} can also accelerate the accumulation of sugar and fiber, and further improve the quality of fruits and cotton (Fujimura *et al.*, 2012). In the DPR, the decreasing DTR, caused by the faster increase in T_{min} than in T_{max}, may reduce crop yields and quality, especially the quality of cotton and fruits. However, the decrease in DTR coincides with the period of rapid fruit and crop production, which can reduce the effect of DTR decrease on agricultural production in the DPR. Climatic warming has shifted crop phenology and affected crop yields. Lobel and Field (2007) showed that global corn yields have a negative correlation with increased temperature. Grain yields have also been shown to have reduced by 35% if T_{max} and T_{min} increase by 1 and 1.5 °C, respectively (Lal *et al.*, 1999). In the western areas of the DPR (sub-regions II and III), more precipitation and glacier melting water will be provided to the oasis agriculture and grassland husbandry, which conversely promotes agricultural development. However, decreasing precipitation in the eastern DPR (sub-region I) may not provide more water to meet the requirements of crop production and grassland productivity, which is not beneficial to crop production and animal husbandry. Some studies have found that grass production has reduced in Inner Mongolia due to decreased precipitation (Li *et al.*, 2013). However, grass production increased due to increased precipitation and temperature in the Three-River source region (Guo, 2013). Due to the complexity of climate change, the impact of precipitation and temperature on agriculture is different. Further research examining the impact of climate trends on crop yields and quality in the different sub-regions of the DPR is therefore necessary to provide a scientific basis for long-term adaption strategies.

5. Conclusions

In this study annual, seasonal and monthly air temperature, precipitation and wind speed trends were examined based on 179 meteorological stations over a period

from 1960 to 2013 using the nonparametric M-K test and Theil-Sen's slope estimator. The results indicated that T_{max}, T_{min}, and T_{mean} have similar positive trends, although T_{min} generally increased at a greater rate than T_{max} for the majority of the months and seasons over the past 54 years. Increasing annual air temperatures were indicated by increases in T_{max}, T_{min}, and T_{mean} of 0.26, 0.44, and 0.33 °C (10 year)$^{-1}$, respectively, but the DTR showed a decrease of 0.19 °C (10 year)$^{-1}$. The majority of meteorological stations recorded increases in air temperature across all timescales. At the same time, most of the meteorological stations recorded a decrease in DTR. Precipitation increased between 1960 and 2013 for the majority of meteorological stations in sub-regions II and III, and decreased in sub-region I, but few of these trends are statistically significant over all timescales. The climate is becoming warmer and wetter in the western areas of the DPR, and warmer and drier in the eastern areas of the DPR. The majority of meteorological stations recorded a significant decrease in WS across almost all timescales, with an annual magnitude of 0.158 m s^{-1} (10 year)$^{-1}$. Better understanding of how the historical climate has been changing will provide scientific support for the adaption of mitigation policies of land desertification/degradation, water resources, ecological projects, and agricultural productions; all of which will aid in combating desertification processes, maintaining ecological security and sustainable development in the DPR.

Acknowledgements

This research was supported by grants from '948' Project of State Forestry Administration P.R. China(2015-4-27), The International S&T Cooperation Program of China (2015DFR31130), and the National Natural Science Foundation of China (41271033; 41471029; 41371500).

References

CCNARCC (Commission of China's National Assessment Report on Climate Change). 2007. *China's National Assessment Report on Climate Change*. Science Press: Beijing.

Chen F, Huang W, Jin L, Chen J, Wang J. 2011. Spatiotemporal precipitation variations in the arid Central Asia in the context of global warming. *Sci. China: Earth Sci.* **54**(12): 1812–1821.

Dai X, Wang P, Zhang K. 2013. A study on precipitation trend and fluctuation mechanism in northwestern China over the past 60 years. *Acta Phys. Sin.* **62**(12): 129201 (In Chinese).

Dai S, Shulski MD, Hubbard KG, Takle ES. 2015. A spatiotemporal analysis of Midwest US temperature and precipitation trends during the growing season from 1980 to 2013. *Int. J. Climatol.* doi: 10.1002/joc.4354.

Ding YH, Wang ZY, Sun Y. 2008. Inter-decadal variation of the summer precipitation in East China and its association with decreasing Asian summer monsoon. Part I: observed evidence. *Int. J. Climatol.* **28**: 1139–1161.

Du J, Ma YC. 2004. Climatic trend of rainfall over Tibetan Plateau from 1971 to 2000. *Acta Geogr. Sin.* **59**(3): 375–382.

Duhan D, Pandey A, Gahalaut KPS, Pandey RP. 2013. Spatial and temporal variability in maximum, minimum and mean air temperatures at Madhya Pradesh in central India. *C. R. Geosci.* **345**: 3–21.

Fan B, Guo L, Li N, Chen J, Lin H, Zhang X, Shen M, Rao Y, Wang C, Ma L. 2014. Earlier vegetation green-up has reduced spring dust storms. *Sci. Rep.* **4**: 6749, doi: 10.1038/srep06749.

Fujimura S, Suzuki K, Nagao M, Okada M. 2012. Acclimation to root chilling increases sugar concentrations in tomato (*Solanum lycopersicum* L.) fruits. *Sci. Hortic.* **147**: 34–41.

Gao J, Liu Y. 2010. Determination of land degradation causes in Tongyu County, Northeast China *via* land cover change detection. *Int. J. Appl. Earth Obs. Geoinf.* **12**(1): 9–16.

Gong DY, Wang SW. 2000. The north Atlantic oscillation index and its interdecadal variability. *Chin. J. Atmos. Sci.* **24**(2): 187–192.

Guo L. 2013. Climatic changes on alpine grassland of the Three-Rivers Source region and their poten tial impacts on grass yield. *Pratacult. Sci.* **30**(10): 1613–1618.

Guo AJ, Chang JX, Huang Q, Sun JN. 2014. Quantitative analysis of the impacts of climate change and human activities on runoff change in Weihe Basin. *J. Northwest Agri. For. Univ. (Nat. Sci. Ed.)* **42**(8): 212–220 (in Chinese).

He W, Bu RC, Xiong ZP, Hu YM. 2013. Characteristics of temperature and precipitation in Northeastern China from 1961 to 2005. *Acta Ecol. Sin.* **33**(2): 519–531.

Hoffman MT, Cramer MD, Gillson L, Wallace M. 2011. Pan evaporation and wind run decline in the Cape Floristic region of South Africa (1974–2005): implications for vegetation responses to climate change. *Clim. Change* **109**: 437–452.

Hua W, Fan G, Wang B. 2012. Variation of Tibetan Plateau summer monsoon and its effect on precipitation in East China. *Chin. J. Atmos. Sci.* **36**(4): 784–794 (in Chinese).

IPCC. 2013. Summary for policymakers. In *Climate Change 2013: The Physical Science Basis. Contribution of Working Group I to the Fifth Assessment Report of the Intergovernmental Panel on Climate Change*, Stocker TF, Qin D, Plattner GK, Tignor M, Allen SK, Boschung J, Nauels A, Xia Y, Bex V, Midgley PME (eds). Cambridge University Press: Cambridge and New York, 37–38.

Japay D, Gang C. 2008. Inter-decadal variation characteristics of wind speed in East Xinjiang. *Arid Meteorol.* **26**(3): 14–21.

Kendall MG. 1975. *Rank Correlation Methods*. Griffin: London.

Lal M, Singh KK, Srinivasan G, Rathore LS, Naidu D, Tripathi CN. 1999. Growth and yield responses of soybean in Madhya Pradesh, India to climate variability and change. *Agric. For. Meteorol.* **93**: 53–70.

Li Z. 2012. Glaciers and lakes changes on the Qinghai-Tibet plateau under climate change in the past 50 years. *J. Nat. Resour.* **27**(8): 1431–1443.

Li X, Liu X, Cao Y. 2013. Research in the climatic change influencing pasture growth in Inner Mongolia grassland. In: *Annual Meeting of the 30th China Meteorological Society on Innovation Driven Development to Improve the Defense Capability of Meteorological Disasters*: *S7 Response to Climate Change and Agricultural Meteorological Disaster Prevention and Mitigation*, 22 October 2013, Nanjing, China.

Li Z, Chen Y, Yang J, Wang Y. 2014. Potential evapotranspiration and its attribution over the past 50 years in the arid region of Northwest China. *Hydrol. Processes* **28**: 1025–1031.

Liu C, Wang H, Jiang D. 2004. The configurable relationships between summer monsoon and precipitation over East Asia. *Chin. J. Atmos. Sci.* **28**(5): 700–712.

Liu S, Ding Y, Li J, Shangguan D, Zhang Y. 2006. Glaciers in response to recent climate warming in western China. *Quat. Sci.* **26**(5): 762–771.

Liu H, Yin Y, Piao S, Zhao F, Engels M, Ciais P. 2013. Disappearing lakes in semiarid northern China: drivers and environmental impact. *Environ. Sci. Technol.* **47**(21): 12107–12114, doi: 10.1021/es305298q.

Lobel DB, Field CB. 2007. Global scale climate-crop yield relationships and the impacts of recent warming. *Environ. Res. Lett.* **2**: 1–7.

Lobell DB. 2007. Changes in diurnal temperature range and national cereal yields. *Agric. For. Meteorol.* **145**(3–4): 229–238.

Lobell DB, Burke MB. 2008. Why are agricultural impacts of climate change so uncertain? The importance of temperature relative to precipitation. *Environ. Res. Lett.* **3**: 1–8.

Lu Y, Wang RH, Cai ZY. 2009. Climatic change and influence in arid and semi-arid area of China. *J. Arid Land Resour. Environ.* **23**(11): 65–71.

Martinez CJ, Maleski JJ, Miller MF. 2012. Trends in precipitation and temperature in Florida, USA. *J. Hydrol.* **452–453**: 259–281.

McVicar TR, Roderick ML, Donohue RJ, Li LT, van Niel TG, Thomas A, Grieser J, Jhajharia D, Himri Y, Mahowald NM, Mescherskaya AV, Kruger AC, Rehman SR, Dinpashoh Y. 2012. Global review and synthesis of trends in observed terrestrial near-surface wind speeds: implications for evaporation. *J. Hydrol.* **416–417**: 182–205.

Najafi MR, Zwiers FW, Gillett NP. 2015. Attribution of Arctic temperature change to greenhouse-gas and aerosol influences. *Nat. Clim. Change* **5**: 246–249.

Ren ZX, Yang DY. 2007. Trend and characteristics of climatic change in Arid region of northwest China in resent 50 years. *J. Earth Sci. Environ.* **29**(1): 99–102.

Sayemuzzaman M, Jha MK. 2014. Seasonal and annual precipitation time series trend analysis in North Carolina, United States. *Atmos. Res.* **137**: 183–194.

Sen PK. 1968. Estimates of the regression coefficient based on Kendall's tau. *J. Am. Stat. Assoc.* **63**: 1379–1389.

Shan N, Shi Z, Yang X, Gao J, Cai D. 2015. Spatiotemporal trends of reference evapotranspiration and its driving factors in the Beijing-Tianjin sand source control project region, China. *Agric. For. Meteorol.* **200**: 322–333.

Song S, Li L, Chen X, Bai J. 2015. The dominant role of heavy precipitation in precipitation change despite opposite trends in west and east of northern China. *Int. J. Climatol.* **35**: 4329–4336, doi: 10.1002/joc.4290.

Sperber K, Annamalai H, Kang IS, Kitoh A, Moise A, Turner A, Wang B, Zhou T. 2013. The Asian summer monsoon: an intercomparison of CMIP5 vs. CMIP3 simulations of the late 20th century. *Clim. Dyn.* **41**: 2711–2744.

Tabari H, Hosseinzadeh Talaee P. 2011. Recent trends of mean maximum and minimum air temperatures in the western half of Iran. *Meteorol. Atmos. Phys.* **111**: 121–131.

Tait A, Woods R. 2007. Spatial interpolation of daily potential evapotranspiration for New Zealand using a spline model. *J. Hydrometeorol.* **8**: 430–438.

Takle ES, Anderson C, Andresen J, Angel JR, Elmore R, Gramig B, Guinan P, Hilberg S, Kluck D, Massey R, Niyogi D, Schneider J, Shulski M, Todey D, Widhalm M. 2014. Climate forecasts for corn producer decision-making. *Earth Interact.* **18**: 1–8.

Tan SC, Shi GY, Wang H. 2012. Long-range transport of spring dust storms in Inner Mongolia and impact on the China seas. *Atmos. Environ.* **46**: 299–308.

Tao S, Fang J, Zhao X, Zhao S, Shen H, Hu H, Tang Z, Wang Z, Guo Q. 2015. Rapid loss of lakes on the Mongolian Plateau. *Proc. Natl. Acad. Sci. USA* **112**(7): 2281–2286.

Trengberth KE, Jones PD, Ambenje P, Bojariu R, Easterling D, Klein Tank A, Parker D, Rahimzadeh F, Renwick JA, Rusticucci M, Soden B, Zhai P. 2007. Observations: surface and atmospheric climate change. In *Climate Change 2007: The Physical Science basis. Contribution of Working Group I to the Fourth Assessment Report of the Intergovernmental Panel on Climate Change*, Solomon S, Qin D, Manning M, Chen Z, Marquis M, Averyt KB, Tignor M, Miller HL (eds). Cambridge University Press: Cambridge, New York.

Tubi A, Dayan U. 2013. The Siberian high: teleconnections, extremes and association with the Icelandic Low. *Int. J. Climatol.* **33**(6): 1357–1366.

Vautard R, Cattiaux J, Yiou P, Thepau JN, Ciais P. 2010. Northern Hemisphere atmospheric stilling partly attributed to an increase in surface roughness. *Nat. Geosci.* **3**: 756–761.

Wang YQ, Zhou L. 2005. Observed trends in extreme precipitation events in China during 1961–2001 and the associated changes in large-scale circulation. *Geophys. Res. Lett.* **32**: L09707.

Wang X, Wang T, Dong Z, Liu X, Qian G. 2006. Nebkha development and its significance to wind erosion and land degradation in semi-arid northern China. *J. Arid Environ.* **65**(1): 129–141.

Wang CZ, Niu SJ, Wang LN. 2010. Spatial and temporal pattern of sand-dust storms in China during 1958–2007. *J. Desert Res.* **30**(4): 933–939.

Wang B, Liu J, Kim HJ, Webster PJ, Yim SY. 2011. Recent change of the global monsoon precipitation (1979–2008). *Clim. Dyn.* **39**: 1123–1135.

Wang W, Zhang G, Li Z. 2015. Study on equilibrium line altitude and its relationship with climate change of Urumqi Glacier No.1 in Tianshan Mountains in recent 52 years. *J. Nat. Resour.* **30**(1): 124–132.

Wu B, Su ZZ, Chen ZX. 2007. A revised potential extent of desertification in China. *J. Desert Res.* **27**(6): 911–917.

Xu M, Chang CP, Fu C, Qi Y, Robock A, Robinson D, Zhang H. 2006. Steady decline of East Asian monsoon winds, 1969–2000: evidence from direct ground measurements of wind speed. *J. Geophys. Res. Atmos.* **111**: D24.

Yang J, Tan C, Zhang T. 2013. Spatial and temporal variations in air temperature and precipitation in the Chinese Himalayas during the 1971–2007. *Int. J. Climatol.* **33**: 2622–2632.

Yu H, Hammond J, Ling S, Zhou S, Mortimer PE, Xu J. 2014. Greater diurnal temperature difference, an overlooked but important climatic driver of rubber yield. *Ind. Crop. Prod.* **62**: 14–21.

Zhang XQ, Ren Y, Yin ZY, Lin ZY, Zheng D. 2009. Spatial and temporal variation patterns of reference evapotranspiration across the Qinghai-Tibetan Plateau during 1971–2004. *J. Geophys. Res.* **114**: D15105.

Zhang SL, Wang YH, Yu PT, Zhang HJ, Liu GF, Tu XW. 2011. Spatio-temporal variance of annual runoff in Jinghe River basin of northwest China in past 50 years and its main causes. *Sci. Geogr. Sin.* **31**(6): 721–727.

Zhao P, Yang S, Yu RC. 2010. Long-term changes in rainfall over Eastern China and large-scale atmospheric circulation associated with recent global warming. *J. Clim.* **23**: 1544–1562.

Zhu GF, He YQ, Pu T, Li ZX, Wang XF, Jia WX, Xin HJ. 2011. Spatial distribution and temporal trends in potential evaporation over Hengduan Mountains region from 1960 to 2009. *Acta Geogr. Sin.* **66**(7): 905–916.

Zhu XF, Zhao AZ, Li YZ, Cao S, Li MY. 2014. Impact of irrigation on climate. *Acta Ecol. Sin.* **34**(17): 4816–4828.

